Journal of Organometallic Chemistry 881 (2019) 34–44

Contents lists available at ScienceDirect

Journal of Organometallic Chemistry

journal homepage: www.elsevier.com/locate/jorganchem

Synthesis of rhenacyclopentadienes and η^2:η^2-diyne complexes from a labile dirhenium carbonyl and π-conjugated 1,7-octadiynes: Structural and photophysical characterization

Claudia Cardozo [a], Axel Mendoza [a], Gabriela Farías [a], André Luiz Barboza Formiga [b], Deisy Peña [a], Franmerly Fuentes [a], Alejandro Arce [a], Yomaira Otero [a], *

[a] *Centro de Química, Instituto Venezolano de Investigaciones Científicas (IVIC), Apartado 21827, Caracas, 1020-A, Venezuela*
[b] *Institute of Chemistry, University of Campinas, P.O. Box 6154, 13083-970, Campinas, Brazil*

ARTICLE INFO

Article history:
Received 4 October 2018
Received in revised form
29 November 2018
Accepted 3 December 2018
Available online 4 December 2018

Keywords:
Dirhenium carbonyls
Fluorescent rhenacyclopentadiene
1,7-octadiynes
π-conjugated diyne
Photophysical properties

ABSTRACT

A series of dirhenium carbonyl compounds containing π-conjugated diyne ligands and symmetrical 2,5-bis(aryl)rhenacyclopentadienes has been synthesized by reaction of $[Re_2(CO)_8(CH_3CN)_2]$ and 1,8-bis(aryl)-1,7-octadiyne derivatives [aryl = 2-thienyl (**a**), 2-pyridyl (**b**), 2-quinolyl (**c**) and 9-phenanthrenyl (**d**)]. We found that diyne ligands undergo coordination to the labile rhenium dinuclear in bridging or chelate modes, however, the formation of metallacyclopentadiene complexes was favorably observed. All products were fully characterized by IR, NMR, ESI-MS, UV–Vis and fluorescence spectroscopy. Single-crystal structures of three new 2,5-bis(aryl)rhenacyclopentadienes $[Re_2(CO)_7(\mu\text{-}\eta^1{:}\eta^1{:}\eta^2{:}\eta^2\text{-}C_{16}H_{14}S_2)]$ (**1a**), $[Re_2(CO)_6(CH_3CN)(\mu\text{-}\eta^1{:}\eta^1{:}\eta^2{:}\eta^2\text{-}C_{16}H_{14}S_2)]$ (**2a**) and $[Re_2(CO)_6(CH_3CN)(\mu\text{-}\eta^1{:}\eta^1{:}\eta^2{:}\eta^2\text{-}C_{26}H_{20}N_2)]$ (**2c**) are described. DFT calculations were used to evaluate the proposed geometries for the two η^2:η^2-diyne complexes $[Re_2(CO)_6(CH_3CN)_2(\mu\text{-}\eta^2{:}\eta^2\text{-}C_{18}H_{16}N_2)]$ (**3b**), $[Re_2(CO)_6(CH_3CN)_2(\eta^2{:}\eta^2\text{-}C_{26}H_{20}N_2)]$ (**4c**), and the rhenacyclopentadiene $[Re_2(CO)_6(CH_3CN)(\mu\text{-}\eta^1{:}\eta^1{:}\eta^2{:}\eta^2\text{-}C_{36}H_{26})]$ (**2d**). The photophysical properties of all complexes were assessed, in that they exhibited fluorescence between 408 and 599 nm with quantum yields of $\Phi_f = 0.02\text{–}0.09$. An exceptional fluorescence quantum yield of $\Phi_f = 0.64$ was found for $[Re_2(CO)_6(CH_3CN)_2(\eta^2{:}\eta^2\text{-}C_{26}H_{20}N_2)]$ (**4c**), which has been attributed to its rigid chelate structure. This work represents the second example of fluorescent 2,5-bis(aryl)rhenaclyclopendadienes reported up to date.

1. Introduction

π–Conjugated systems have been of interest for many scientists owing to their numerous applications in the field of material science, involving photochemical and photobiological processes [1–10]. π–Conjugated diynes have been useful building blocks for industrial intermediates and starting materials in the synthesis of conjugated polymers, liquid crystals, molecular wires, nonlinear optic materials, natural products, pharmaceutical and bioactive compounds, among others [11–20].

In organometallic chemistry, diynic compounds offer a number of coordination modes and reactivity patterns with transition metal carbonyls [21–28] that often result in η^2-alkyne complexes or interesting metallacyclic compounds, such as metallacyclopentadienes [19,29–35]. Since the first metallacyclopentadiene was successfully synthesized in 1958 [36], they have received considerable attention because of its unique metallacyclic structure [37–42], and different synthetic methods have been reported [27,34,37,43–49]. They are well-known as intermediates in a diversity catalytic cyclotrimerization reactions [39,48], but very little have been reported about the photophysical properties of substituted metallacyclopentadienes [44,50–55].

In 2001, Marder and co-workers successfully developed a high-yield one-pot synthesis of luminescent 2,5-bis(arylethynyl)rhodacyclopentadienes by reductive coupling of 1,4-diarylbuta-1,3-diynes, and since then, a variety of 1,4-bis(*p*-R-phenyl)-1,3-butadiynes and 1,8-bis(*p*-R-phenyl)-1,7-octadiynes have been used to develop a family of this class of rhodacyclopentadienes [55–57]. Depending on the aryl substituents, these 2,5-bis(arylethynyl)rhodacyclopentadienes can exhibit fluorescence

---

* Corresponding author.
E-mail address: yotero@ivic.gob.ve (Y. Otero).

https://doi.org/10.1016/j.jorganchem.2018.12.003

with quantum yields of $\Phi_f = 0.01–0.69$ [53,56,57]. Likewise, 2,5-bis(*p*-$MeO_2C-C_6H_4-C{\equiv}C$)iridacyclopenta-2,4-diene was also reported, this metallacycle displays fluorescence with $\Phi_f = 0.08$ and no visible phosphorescence, despite of the presence of the heavy atom [53].

Herein, we have studied the reaction of $[Re_2(CO)_8(CH_3CN)_2]$ with four 1,8-bis(aryl)-1,7-octadiyne derivatives [aryl = 2-thienyl (**a**), 2-pyridyl (**b**), 2-quinolyl (**c**) and 9-phenanthrenyl (**d**)] for the preparation of 2,5-bis(aryl)rhenacyclopentadienes and η^2:η^2-diyne complexes. Their spectroscopy characterization and photophysical properties are described.

2. Results and discussion

2.1. Synthesis and characterization

All dirhenium carbonyl complexes were synthesized by thermal treatment of $[Re_2(CO)_8(CH_3CN)_2]$ with the corresponding diyne derivative [1,8-bis(2-thienyl)octa-1,7-diyne (**a**), 1,8-bis(2-pyridyl) octa-1,7-diyne (**b**), 1,8-bis(2-quinolyl)octa-1,7-diyne (**c**) and 1,8-bis(9-phenanthrenyl)octa-1,7-diyne (**d**)] in refluxing cyclohexane (Scheme 1). In general, we have found that rhenacyclopentadienes were predominantly obtained. Bridging and chelate coordination modes were only observed with 1,8-bis(2-pyridyl)octa-1,7-diyne and 1,8-bis(2-quinolyl)octa-1,7-diyne, respectively. The chelate complex was found to be an intermediate for the formation of corresponding rhenacyclopentadiene.

Reaction of $[Re_2(CO)_8(CH_3CN)_2]$ with 1,8-bis(2-thienyl)octa-1,7-diyne (**a**) gave two dinuclear compounds, characterized as $[Re_2(CO)_7(\mu\text{-}\eta^1{:}\eta^1{:}\eta^2{:}\eta^2\text{-}C_{16}H_{14}S_2)]$ (**1a**) and $[Re_2(CO)_6(CH_3CN)(\mu\text{-}\eta^1{:}\eta^1{:}\eta^2{:}\eta^2\text{-}C_{16}H_{14}S_2)]$ (**2a**), where **1a** was formed by carbonylation of **2b** (exchange of an acetonitrile by a CO ligand).

The carbonyl stretching region in the infrared spectrum for compound **1a** was very similar to that found for related rhenium complexes [29,31,33]. In the ^1H NMR spectrum, the thienyl protons were like the corresponding ones in the free ligand, while the CH_2 protons were no longer found to be chemically equivalent. The $^{13}C\{^1H\}$ NMR spectrum showed equally shifted acetylenic carbons to downfield with respect to the free ligand, due to symmetric coordination of 1,8-bis(2-thienyl)octa-1,7-diyne through both $C{\equiv}C$ bonds. The MS spectrum of **1a** displayed a peak at *m/z* 838.84, which matches with the molecular ion $[M{+}H]^+ = [Re_2(CO)_7(C_{16}H_{14}S_2)]^+$. The observed isotopic pattern ($^{187}Re\text{-}^{185}Re$, $^{185}Re\text{-}^{185}Re$ and $^{187}Re\text{-}^{187}Re$; *m/z* 836.82, 838.84 and 840.83 respectively) was characteristic of rhenium dinuclear complexes [58] The molecular structure of **1a** was established by single-crystal XRD after slow-evaporation recrystallization in cyclohexane/dichloromethane mixture (Fig. 1, Table 1). The molecular structure clearly showed a rhenacyclopentadiene unit that is η^2:η^2-coordinated to a second rhenium atom. Three CO ligands are attached to Re1 and four CO ligands to Re2. The diyne ligand is behaving as a six-electron donor, and each rhenium atom has the optimal 18-valence electron configuration. The Re–C and C–C bond lengths of the rhenacyclopentadiene ring [Re1–C14 = 2.218(4); Re1–C15 = 2.207(4); C14–C8 = 1.413(5); C8–C9 = 1.473(4); C9–C15 = 1.405(5)] are very similar to those reported for analogue complexes [29,31,33]. The Re–Re distance is 2.8821(3) Å, comparable to Re–Re distance values for dinuclear rhenium complexes [29,31,33].

2a displayed a characteristic IR spectrum of hexacarbonyl dinuclear compounds [59–61]. Its ^1H NMR spectrum did not show significant differences in comparison to the free ligand, except for the CH_2 protons that were no longer symmetrical. In the $^{13}C\{^1H\}$ NMR spectrum, the signals assigned to the acetylenic groups are notably downfield shifted, which was indicative of coordination to a metal center as found for **1a**. NMR spectra also revealed the presence of one acetonitrile ligand. The mass spectrum showed a peak at *m/z* 712.82 corresponding to the molecular ion $[M{-}(CO)_5 + H]^+$ ($M = Re_2C_{24}H_{17}S_2O_6N$). Fortunately, we were able to confirm the structure of **2a** by single crystal XRD analysis (Fig. 1, Table 1). The solid-state structure of **2a** revealed a rhenacyclopentadiene complex, which is also η^2:η^2coordinated to a second Re atom as described for **1a**. In contrast to **1a**, an acetonitrile molecule is binding to Re(1) and each rhenium atom has three CO ligands. The Re–C and C–C distances of the metallacyclopentadiene ring [Re1–C14 = 2.186(2); Re1–C15 = 2.188(2); C14–C8 = 1.401(3); C8–C9 = 1.466(4); C9–C15 = 1.404(3)] and Re–Re bond [2.8538(4) Å] are close to those found for **1a** and related compounds [29,31,33].

DFT calculations were used to investigate the geometries obtained by single crystal XRD analysis of **1a** and **2a**. As shown in Figure S1, the superposition of the calculated and experimental structures is in very good agreement. The root-mean-square deviation (RMSD) for **1a** is 0.353 Å when all atoms are considered and 0.168 Å when only the rhenium centers and their bonded atoms are considered. For **2a**, RMSD is 0.477 Å (all atoms) and 0.142 Å (rhenium centers and their bonded atoms). The main differences between calculated and experimental geometries were the conformations of the thienyl groups, since the DFT calculations were performed under vacuum conditions without taking into account the packing effects present in the crystals.

The main product from the reaction of $[Re_2(CO)_8(CH_3CN)_2]$ and 1,8-bis(2-pyridyl)octa-1,7-diyne (**b**) was characterized as $[Re_2(CO)_6(CH_3CN)_2(\mu\text{-}\eta^2{:}\eta^2\text{-}C_{18}H_{16}N_2)]$ (**3b**). Its IR spectrum was very similar to that found for **2a** and related hexacarbonyl dinuclear

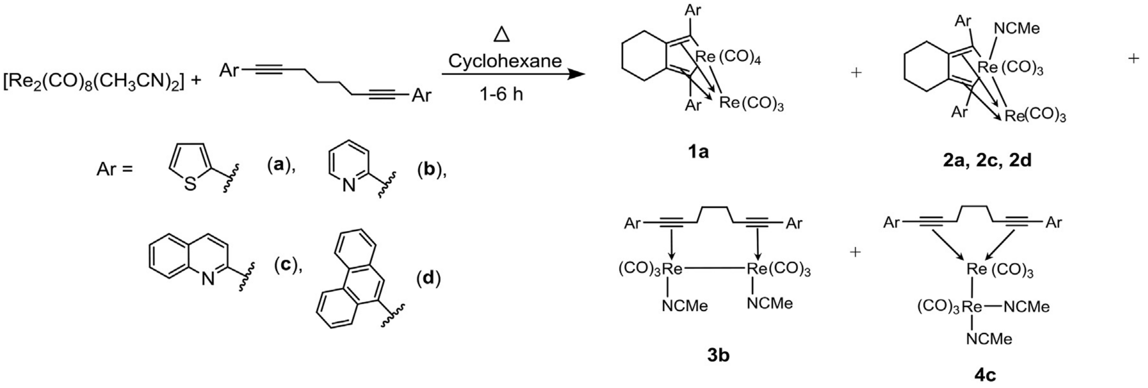

Scheme 1. Reaction of $[Re_2(CO)_8(CH_3CN)_2]$ with π-conjugated 1,7-octadiynes.

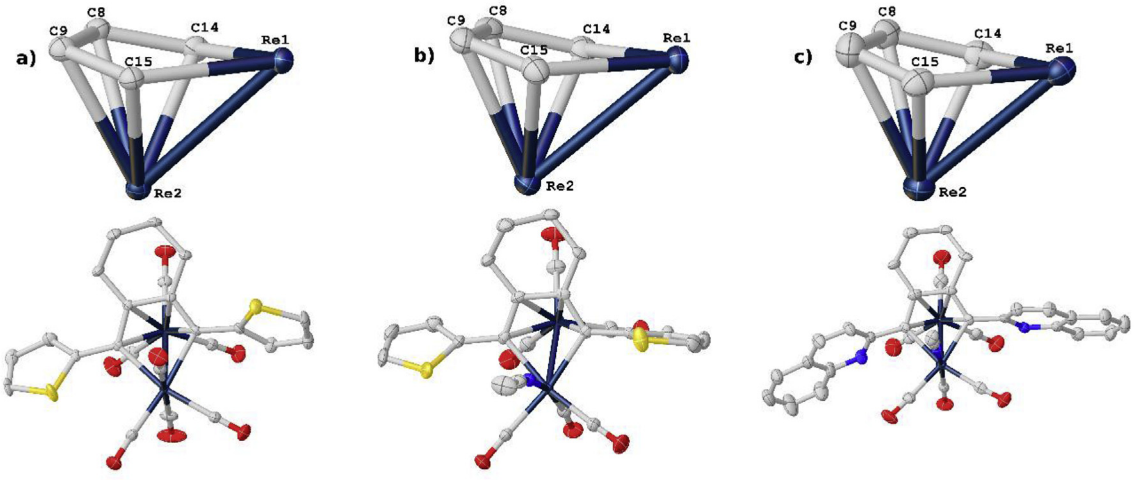

Fig. 1. Molecular structures of complexes a) **1a**, b) **2a** and c) **2c** obtained by single crystal XRD. Details of Re1 and Re2 coordination environments are presented for each complex. Atomic displacement ellipsoids are at the 50% probability level and hydrogen atoms were omitted for clarity.

Table 1
Crystallographic data for complexes **1a**, **2a** and **2c**.

	1a	2a	2c
Chemical formula	$C_{23}H_{14}O_7Re_2S_2$	$C_{24}H_{17}NO_6Re_2S_2$	$C_{34}H_{23}N_3O_6Re_2\cdot 0.4(C_6H_{12})$
Molecular weight (g mol^{-1})	838.86	851.90	975.61
Temperature (K)	150	150	150
Wavelength (Å)	Mo $K\alpha$ 0.71073	Mo $K\alpha$ 0.71073	Mo $K\alpha$ 0.71073
Crystal system	Monoclinic	Monoclinic	Monoclinic
Space group	*Cc*	$P2_1/n$	$C2/c$
a (Å)	9.4716(6)	11.7926(10)	34.655(2)
b (Å)	15.9487(11)	13.1044(11)	8.3341(5)
c (Å)	15.5891(13)	16.8730(15)	26.0969(16)
β (°)	95.693(2)	101.444(2)	99.325(1)
V ($Å^3$)	2343.3(3)	2555.6(4)	7437.7(8)
Z	4	4	8
$\rho_{calcd.}$ (g cm^{-3})	2.378	2.214	1.743
F(000)	1560	1592	3722
μ (mm^{-1})	10.54	9.67	6.55
θ range (°)	2.5–28.3	2.5–27.4	2.4–27.1
Reflections collected/independent	16,517/5542	54,743/5828	48,730/8208
R_{int}	0.017	0.030	0.056
Data/restraints/parameters	5542/142/363	5828/105/382	8208/66/474
$R[F^2 > 2\sigma(F^2)]$, $wR(F^2)$	0.011, 0.022	0.014, 0.030	0.032, 0.066
Diff. peak and hole (e $Å^{-3}$)	0.45, −0.44	0.91, −0.38	0.78, −0.80
Goodness-of-fit on F^2	0.77	1.03	1.05
Flack parameter	0.005(3)		
CCDC number	1831209	1831210	1831211

complexes previously reported [59–61]. The simplicity of the ^{1}H and ^{13}C{^{1}H} NMR spectra suggested a symmetric coordination of diyne ligand with inequivalence of the CH_2 protons. A significant shift of the acetylenic carbons to downfield was observed in the ^{13}C{^{1}H} NMR spectrum, indicating the coordination by the triple bonds. Two acetonitrile molecules are also evidenced by NMR data. The MS spectrum of **3b** displayed a peak at *m/z* 836.31 corresponding to the molecular ion $[M{-}(CH_3CN)_2 + Cl]^-$ ($M = Re_2C_{26}H_{19}O_6N_3$), consistent with the proposed complex. The isotopic contributions ^{185}Re-^{187}Re-^{35}Cl, ^{187}Re-^{187}Re-^{35}Cl and ^{187}Re-^{187}Re-^{37}Cl (*m/z* 836.31, 838.30 and 840.23 respectively) were similar to the observed for $[Re_2(O_2C_2H_3)_2Cl_4\cdot 2H_2O]$ [62]. Unfortunately, we were unable to obtain suitable crystals of **3b** for XRD analysis. However, based on the NMR, IR and MS data, we proposed $[Re_2(CO)_6(CH_3CN)_2(\mu\text{-}\eta^2\text{:}\eta^2\text{-}C_{18}H_{16}N_2)]$ as the molecular structure of **3b** (Scheme 1). DFT calculations were carried out to investigate the proposed geometry and its relative stability. The optimized structure was in good agreement with our estimations (Fig. 2), indicating that a μ-η^2:η^2-coordination is possible with two acetonitrile molecules in equatorial positions. The coordination of both acetylenic groups is only possible with a torsion of the alkyl chain, leading to chemical inequivalence among the CH_2 groups in ^{1}H NMR. As expected, a decrease of the C–C bond order was observed for both acetylenic groups in **3b**.

Thermolysis of **3b** in cyclohexane and *n*-octane was carried out with the aim of obtaining the corresponding rhenacyclopentadiene, but only decomposition of **3b** was observed.

1,8-Bis(2-quinolyl)octa-1,7-diyne (**c**) reacted with $[Re_2(CO)_8(CH_3CN)_2]$ to afford two compounds that were characterized as $[Re_2(CO)_6(CH_3CN)(\mu\text{-}\eta^1\text{:}\eta^1\text{:}\eta^2\text{:}\eta^2\text{-}C_{26}H_{20}N_2)]$ (**2c**) and $[Re_2(CO)_6(CH_3CN)_2(\eta^2\text{:}\eta^2\text{-}C_{26}H_{20}N_2)]$ (**4c**). Thermolysis of **4c** in cyclohexane for 10 h led to the formation of **2c**. As expected, the chelate coordination mode results to be an intermediate during the formation of rhenacyclopentadienic complexes [47,51,63], and that

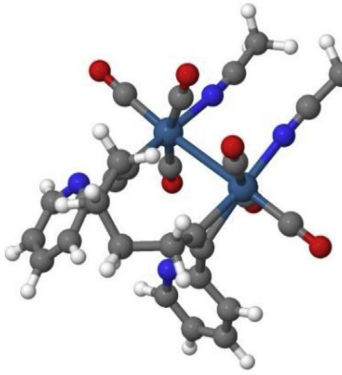

Fig. 2. PBE0/def2-SVP optimized geometries for complex **3b**. Rhenium in cyan, carbon in gray, oxygen in red, nitrogen in blue and hydrogen in white. (For interpretation of the references to colour in this figure legend, the reader is referred to the Web version of this article.)

explains the low yield of **4c** (10%).

The IR υ(CO) frequencies for **2c** were closely related to **2a, 3b** and similar hexacarbonyl dirhenium complexes [59–61]. By comparison with **2a** and **3b**, NMR data of **2c** suggested the formation of a symmetrical rhenacyclopentadiene ring. The presence of an acetonitrile molecule was also evidenced. MS data was consistent with the expected molecular ion $C_{36}H_{26}N_3O_6Re_2$, *m/z:* 942.05 $[M+H]^+$. The single-crystal XRD structure of **2c** (Fig. 1) resulted to be identical to the one described for **2a**. The Re–C and C–C distances [Re1–C14 = 2.179(5), Re1–C15 = 2.176(5), C14–C8 = 1.400(7), C8–C9 = 1.461(8), C9–C15 = 1.412(7)] and Re–Re bond [2.8514(7) Å] were similar to the values found for **1a** and **2a** (Table 1). The calculated geometry of **2c** obtained by DFT was in very good agreement with the experimental molecular structure, thus RMSD is 0.606 (all atoms) and 0.045 Å (rhenium coordination spheres).

The IR υ(CO) frequencies of **4c** suggested a hexacarbonyl dirhenium complex. In ^{1}H NMR, the proton H_3 (at the β-position with respect to the nitrogen atom) is significantly downfield shifted with respect to the free ligand. The rest of the aromatic resonances did not show significant differences, while CH_2 protons were chemically inequivalent. In the $^{13}C\{^1H\}$ NMR spectrum, the acetylenic carbons were notably downfield shifted due to the symmetrical coordination of the triple bonds to the metal center. The presence of two acetonitrile molecules was also evidenced by NMR. The MS spectrum of **4c** displayed a molecular ion $[M-H]^+$ at *m/z* 980.63, which is consistent with the molecular formula $C_{36}H_{26}N_4O_6Re_2$. The available data and previously reported results [64] suggested that the chelate structure shown for **4c** (Scheme 1) is the most likely. The DFT optimized geometry can be seen in Fig. 3. However, this structure differs from the previous ones since the final geometry does not show neither the cyclic six-membered group nor the direct bonding from the ethynyl carbons to the second rhenium fragment. This is probably the reason why a second acetonitrile molecule completes the coordination sphere of the rhenium atom. The predicted Re-Re distance is 3.18 Å the longest one found in this study.

Finally, the reaction of 1,8-bis(9-phenanthrenyl)octa-1,7-diyne (**d**) with $[Re_2(CO)_8(CH_3CN)_2]$ in refluxing cyclohexane afforded only one compound that was characterized as $[Re_2(CO)_6(CH_3CN)(\mu\text{-}\eta^1\text{:}\eta^1\text{:}\eta^2\text{:}\eta^2\text{-}C_{36}H_{26})]$ (**2d**). Its IR and NMR data were very similar to those explained for **2a** and **2c**. The MS spectrum showed a peak at *m/z* 1074.15, corresponding to the molecular ion [M + Cl–H] ($M = Re_2C_{44}H_{29}O_6N$). The DFT optimized geometry resulted in the same coordination mode of **1a** and **2c** as shown in Fig. 4. In this case, the Re–C and C–C bond lengths of the rhenacyclopentadiene ring were Re1–C14 = 2.20 Å, Re1–C15 = 2.22 Å, C14–C8 = 1.40 Å, C8–C9 = 1.47 Å and C9–C15 = 1.41 Å in very close proximity with corresponding lengths obtained by crystallography and DFT for **1a** and **2c**. The calculated Re–Re distance was 2.86 Å.

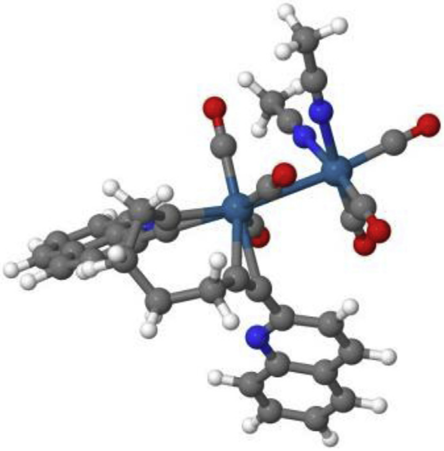

Fig. 3. PBE0/def2-SVP optimized geometries for complexes **4c**. Rhenium is shown in cyan, carbon in gray, oxygen in red, nitrogen in blue and hydrogen in white. (For interpretation of the references to colour in this figure legend, the reader is referred to the Web version of this article.)

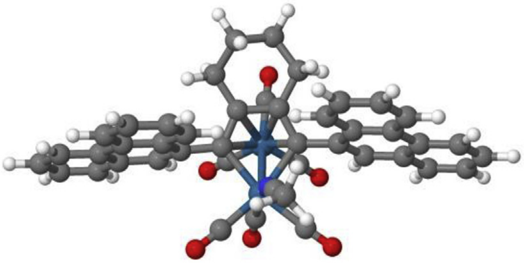

Fig. 4. PBE0/def2-SVP optimized geometries for complex **2d**. Rhenium is shown in cyan, carbon in gray, oxygen in red, nitrogen in blue and hydrogen in white. (For interpretation of the references to colour in this figure legend, the reader is referred to the Web version of this article.)

2.2. Photophysical properties

Diynes ligands and their complexes were analyzed by UV–Vis and fluorescence spectroscopy to evaluate and compare their electronic properties. The spectroscopic data are summarized in Table 2. UV–Vis and fluorescence spectra are shown in Figs. 5 and 6, respectively. The λ_{max} absorption wavelengths are within the range of 230–400 nm while the λ_{max} of emissions are in the region of 359–599 nm.

UV–Vis spectra showed that all complexes present π → π* transitions similar to those originally observed in the ligand molecules, which are slightly blue shifted (Fig. 5), probably due to the presence of electron-rich metal centers in these complexes. The extinction coefficients of all complexes show very different values with respect to their free ligands, indicating that the nature of their transitions has changed upon coordination (Table 2). TD-DFT calculations revealed that these transitions may be better described as Metal-to-Ligand Charge Transfer (MLCT). The density difference plots for these electronic states (Figure S4) displayed negative density differences over the Re atoms and positive density differences over carbonyl and aromatic ligands in all complexes,

Table 2
UV–Vis and fluorescence spectra of diyne ligands and their complexes.

Compound	UV–Vis λ_{max}/nm[a]	TD-DFT λ/nm	ε/M^{-1} cm^{-1}	F λ_{max}/nm[b]	Φ_f[c]	Stokes Shift Δ λ
a	273	–	11892	390	0.12	117
b	295	–	13958	598	0.16	303
c	251	–	155824	359	0.08	108
d	260	–	133286	380	0.17	120
1a	234	233	17384	549	0.09	315
2a	231	237	18163	545	0.06	314
2c	230	235	114960	408	0.06	178
2d	250	247	54300	428	0.03	178
3b	298	294	1828	599	0.02	301
4c	400	409	20540	472	0.64	72

[a] At room temperature in CH_2Cl_2.

[b] At room temperature in CH_2Cl_2. [**a**] = 10^{-5} M, [**b**] = 10^{-5} M, [**c**] = 10^{-6} M, [**d**] = 10^{-6} M, [**1a**] = 10^{-5} M, [**2a**] = 10^{-5} M, [**3b**] = 10^{-4} M, [**2c**] = 10^{-6} M, [**4c**] = 10^{-6} M and [**2d**] = 10^{-6} M.

[c] Fluorescence quantum yield in CH_2Cl_2 relative to tetraphenylporphyrin (Φ_f = 0.11).

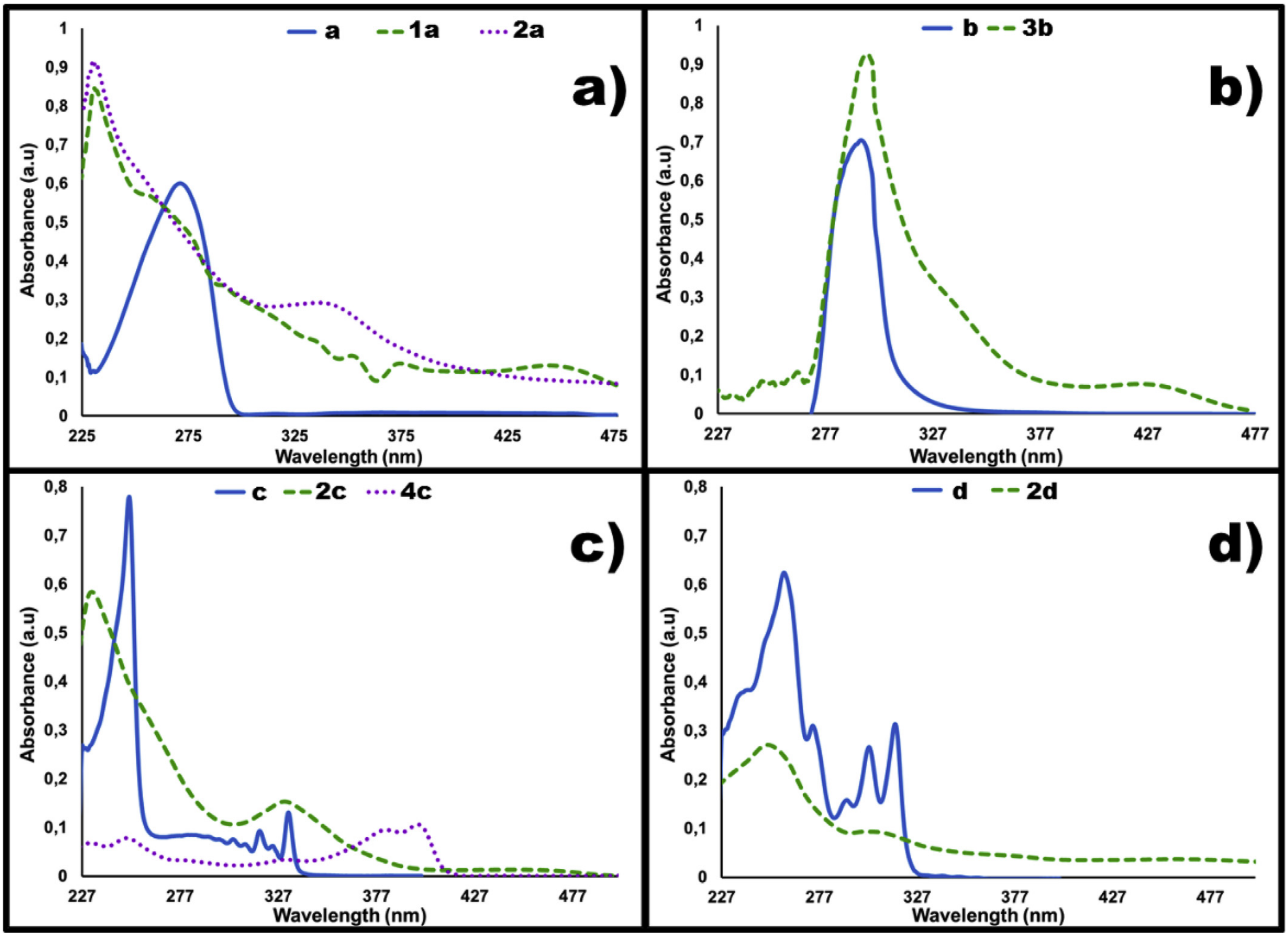

Fig. 5. UV–Vis absorption spectra in CH_2Cl_2 at room temperature for: a) **a**, **1a**, **2a** ([C] = 10^{-5} M); b) **b** ([C] = 10^{-5} M), **3b** ([C] = 10^{-4} M); c) **c**, **2c**, **4c** ([C] = 10^{-6} M); d) **d**, **2d** ([C] = 10^{-6} M).

supporting their assignment as MLCT. The predicted energies of all complexes are in very good agreement with those experimentally obtained, as shown in Table 2 (see also Figure S3).

Fluorescence spectra have shown that diyne ligands and their corresponding complexes exhibit emission between 359 and 599 nm (Fig. 6). Compound **4c** unveiled a broad emission spectrum with an additional band at 472 nm (Fig. 6c), which might be assigned to a MLCT transition state involving a low-lying π^* orbital of the ligand [65–71].

As summarized in Table 2 and Fig. 7, a wide range of Stokes shifts were found for all complexes, where rhenacyclopentadienes **1a** and **2a** displayed the largest Δλ values (315 and 314 nm, respectively). **4c**, possessing a chelated octa-1,7-diyne ligand, presented the shorter Stokes shift in this study (Δλ = 72 nm). This suggests that

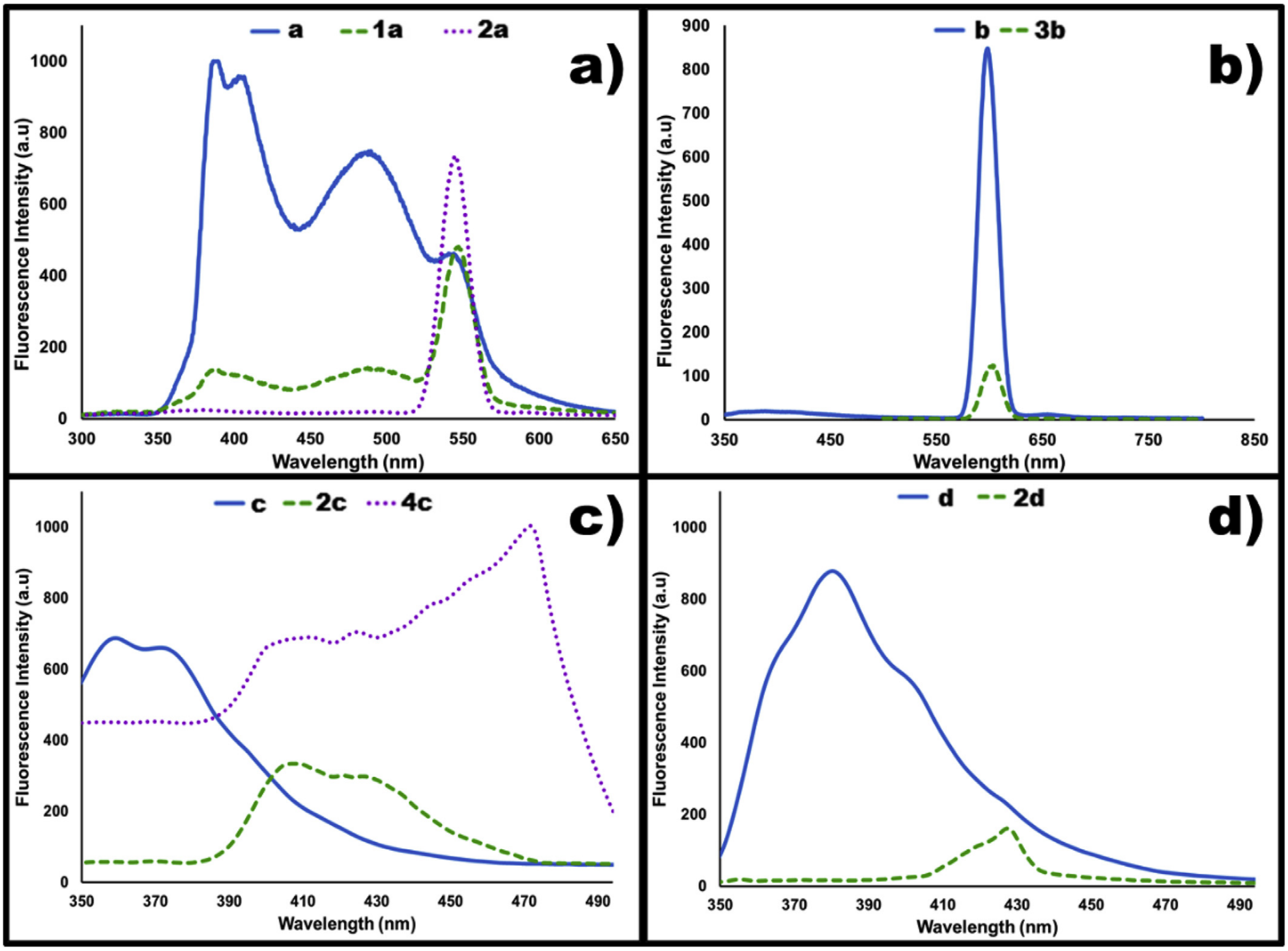

Fig. 6. Emission spectra in CH_2Cl_2 at room temperature for: a) **a**, **1a**, **2a** ([C] = 10^{-5} M); b) **b** ([C] = 10^{-5} M), **3b** ([C] = 10^{-4} M); c) **c**, **2c**, **4c** ([C] = 10^{-6} M); d) **d**, **2d** ([C] = 10^{-6} M).

the fluorescence of **4c** occurs from the excited singlet state S_1, despite that carbon atoms are directly bound to a heavy metal atom, similar to found for iridium and rhodium complexes with rigid structures [53,56].

Rhenacyclopentadienes **1a**, **2a**, **2c** and **2d** exhibited fluorescence with quantum yields of $\Phi_f = 0.03–0.09$, being these Φ_f values comparable to those reported for related rhodacyclopentadienes ($\Phi_f = 0.01–0.69$) [50,53–55,57]. The analysis of the frontier Kohn-Sham orbitals showed similarities between the two series of metallacyclopentadienes. In all cases, electron delocalization from $Re(CO)_n$ fragments to the ligand molecules is observed but in different degrees. Orbital plots can be seen in Figure S2 and a molecular orbital diagram for the rhenacyclopentadienes in this work can be seen in Fig. 8. The energy separation between HOMO-LUMO orbitals is high, ranging from 3.77 to 4.02 eV. Moreover, the frontier orbitals are energetically isolated from the other orbitals, especially the LUMO. The same trends were observed in the rhodacyclopentadiene series reported by Marder and collaborators in which energy separations were calculated in the 2.71–2.91 eV range for the HOMO-LUMO gap [53]. Another similarity between the electronic structures of the two series is the relative low weigh of the heavy atom in the frontier orbitals, more importantly for the LUMO. A combination of these two characteristics associated with the rigidity of the ligands explain the presence of fluorescence in these compounds as a consequence of a lower than expected spin-orbit coupling for the compounds [53].

Thus, the rhenacyclopentadienes reported in this study represent the second family of fluorescent 2,5-disubstituted metallacyclopentadienes reported in the literature [50,53–55,57], although phosphorescence would have been expected due to the heavy atom effect [72–78]. Likely, additional vibrational modes in the complexes generate new ways of non-radiative decay and are thus responsible for lower quantum yields compared to their free ligands (Table 2) [55,70]. For complex **4c**, the fluorescence quantum yield ($\Phi_f = 0.64$) was significantly higher with respect to the free ligand ($\Phi_f = 0.08$), possibly due to the more rigid structure by the chelated diyne ligand [53,56,79].

3. Conclusions

The labile dinuclear $[Re_2(CO)_8(CH_3CN)_2]$ reacts with a variety of 1,8-bis(aryl)-1,7-octadiyne derivatives [aryl = 2-thienyl (**a**), 2-pyridyl (**b**), 2-quinolyl (**c**) and 9-phenanthrenyl (**d**)], leading to new π-complexes. We found that the formation of 2,5-disubstituted metallacyclopentadiene complexes was favored. When 1,8-bis(2-quinolyl)-1,7-octadiyne was used a chelate complex (**4c**) was also obtained, which was found to be an intermediate in the formation of the corresponding rhenacyclopentadiene. It was not possible to isolate the expected metallacycle from reaction of $[Re_2(CO)_8(CH_3CN)_2]$ with 1,8-bis(2-pyridyl)octa-1,7-diyne (**b**), only

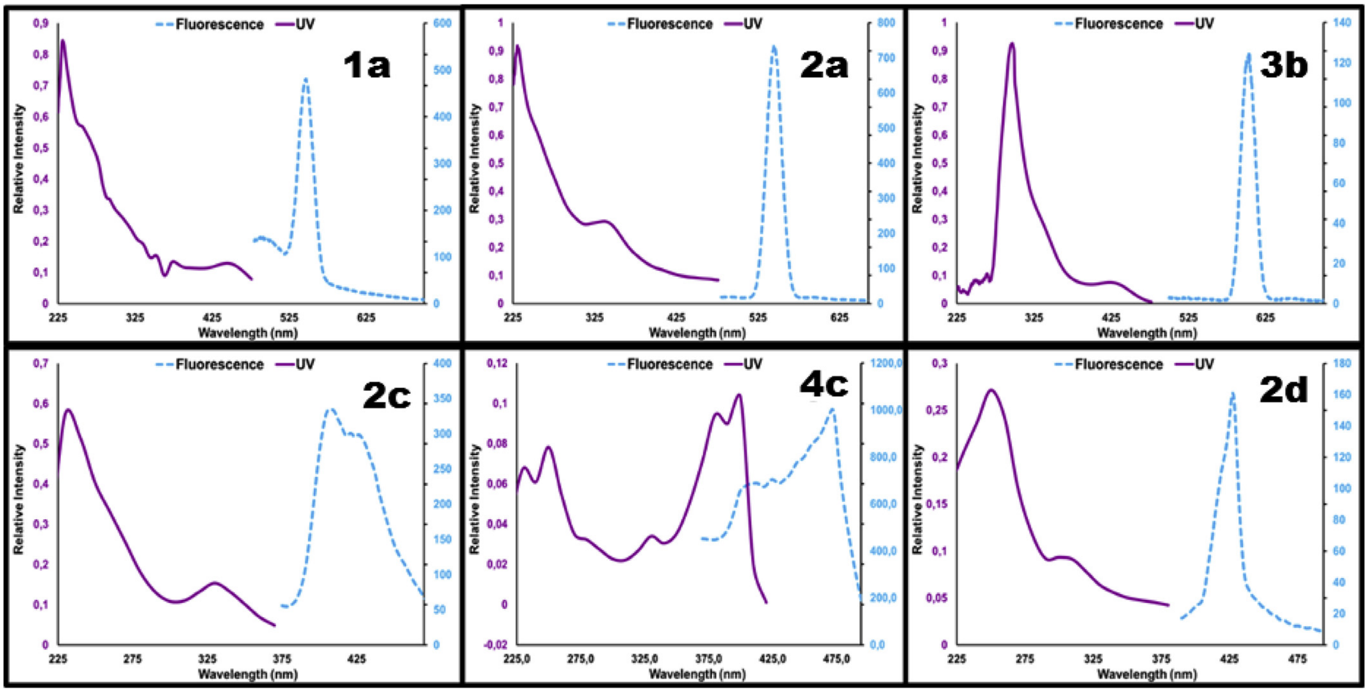

Fig. 7. UV–Vis absorption and fluorescence spectra of all complexes in CH_2Cl_2 at room temperature. **1a**, **2a** ([C] = 10^{-5} M), **3b** ([C] = 10^{-4} M), **2c**, **4c** ([C] = 10^{-6} M), **2d** ([C] = 10^{-6} M).

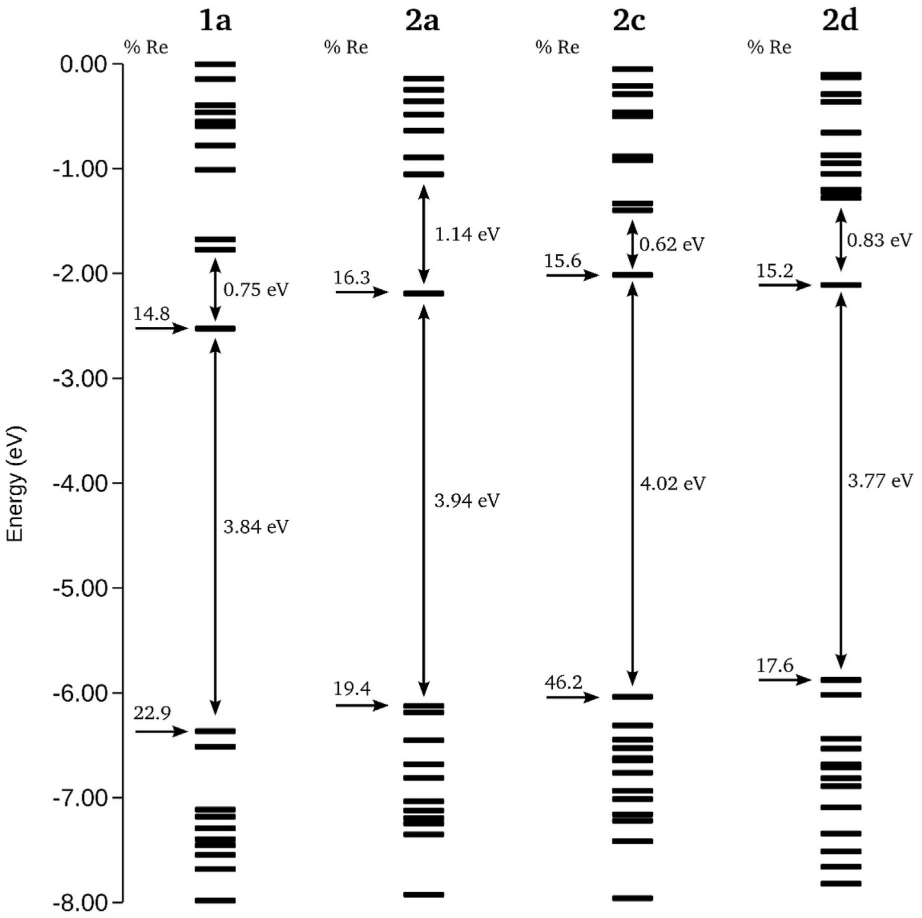

Fig. 8. Molecular orbital diagrams for the series of rhenacyclopentadienes 1a, 2a, 2c and 2d. Horizontal arrows indicate the HOMO and LUMO orbitals and their corresponding contribution from Re atoms in each of these orbitals. Vertical arrows indicate energy separations between orbitals.

a bridge π-coordination of the diyne ligand was observed (complex **3b**).

DFT calculations accurately supported the experimental results obtained by single-crystal XRD. DFT calculations were also used to evaluate the proposed geometries of $[Re_2(CO)_6(CH_3CN)(\mu\text{-}\eta^1{:}\eta^1{:}\eta^2{:}\eta^2\text{-}C_{36}H_{26})]$ (**2d**), $[Re_2(CO)_6(CH_3CN)_2(\mu\text{-}\eta^2{:}\eta^2\text{-}C_{18}H_{16}N_2)]$ (**3b**), and $[Re_2(CO)_6(CH_3CN)_2(\eta^2{:}\eta^2\text{-}C_{26}H_{20}N_2)]$ (**4c**). The photophysical studies showed that all complexes exhibit fluorescence with quantum yields $\Phi_f = 0.02$–0.64, despite the presence of heavy atoms. The chelate complex **4c**, with a more rigid structure, presented the higher quantum yield ($\Phi_f = 0.64$). Lastly, the rhenacyclopentadienes reported in this study represent the second family of fluorescent 2,5-disubstituted metallacyclopentadienes.

4. Experimental section

4.1. General Remarks

All reactions were carried out under an argon atmosphere using standard Schlenk techniques unless otherwise stated. The solvents were previously dried and distilled following standard methods [80]. $[Re_2(CO)_8(CH_3CN)_2]$, 1,8-bis(2-thienyl)octa-1,7-diyne (**a**); 1,8-bis(2-pyridyl)octa-1,7-diyne (**b**); 1,8-bis(2-quinolyl)octa-1,7-diyne (**c**); and 1,8-bis(9-phenanthrenyl)octa-1,7-diyne (**d**) were synthesized according to published procedures [81–83]. ^1H and ^{13}C NMR spectra were recorded using Bruker Avance AM300, AM500 and AM600 spectrometers and assignment of carbon chemical shifts was based on HMBC and HMQC experiments. Infrared spectra were recorded as cyclohexane and CH_2Cl_2 solutions using a 2 mm CaF_2 cell on a Spectrum 100 series Perkin Elmer spectrophotometer. Mass spectra were acquired on a Thermo Scientific TSQ Quantum Ultra AM Triple Quadrupole mass spectrometer employing the Heated Electrospray Ionization (HESI) technique. The UV−Vis spectra were performed on a PerkinElmer Lambda 2 spectrophotometer. Fluorescence spectra were recorded at room temperature on a Perkin Elmer LS45 fluorescence spectrometer with a pulse xenon lamp. Fluorescence quantum yields (Φ_f) were determined in CH_2Cl_2 on freshly prepared samples (air-equilibrated) with absorbance at the excitation wavelength (417 nm for the standard tetraphenylporphyrin). Solutions of tetraphenylporphyrin in CH_2Cl_2 were used as a standard ($\Phi_f = 0.11$).

4.2. Synthesis of $[Re_2(CO)_7(\mu\text{-}\eta^1{:}\eta^1{:}\eta^2{:}\eta^2\text{-}C_{16}H_{14}S_2)]$ (1a) and $[Re_2(CO)_6(CH_3CN)(\mu\text{-}\eta^1{:}\eta^1{:}\eta^2{:}\eta^2\text{-}C_{16}H_{14}S_2)]$ (2a)

A solution of $[Re_2(CO)_8(CH_3CN)_2]$ (100 mg, 0.147 mmol) and 1,8-bis(2-thienyl)octa-1,7-diyne (**a**) (38 mg, 0.147 mmol) in cyclohexane (25 mL) was stirred and refluxed for 1 h under nitrogen. The solvent was evaporated to dryness, and the solid residue was chromatographed by TLC (SiO_2, eluant: hexane/dichloromethane, 8:2 v/v) to give $[Re_2(CO)_7(\mu\text{-}\eta^1{:}\eta^1{:}\eta^2{:}\eta^2\text{-}C_{16}H_{14}S_2)]$ (**1a**) (16 mg; yield 17%) and $[Re_2(CO)_6(CH_3CN)(\mu\text{-}\eta^1{:}\eta^1{:}\eta^2{:}\eta^2\text{-}C_{16}H_{14}S_2)]$ (**2a**) (15 mg; yield 12%). Spectral data for **1a**: IR (cyclohexane, $\nu_{(CO)}/cm^{-1}$): 2087 m, 2034 s, 2017 m, 1978 s, 1965 w, 1935 m. ^1H NMR (600 MHz, $CDCl_3$): δ 7.17 (dd, 2H, $^3J_{H5\text{-}H4} = 5.4$ Hz, $^4J_{H5\text{-}H3} = 1.0$ Hz, $H_{5\ Thienyl}$), 6.95 (dd, 2H, $^3J_{H4\text{-}H5} = 5.4$ Hz, $^3J_{H4\text{-}H3} = 3.6$ Hz, $H_{4Thienyl}$), 6.72 (dd, 2H, $^3J_{H3\text{-}H4} = 3.6$ Hz, $^4J_{H3\text{-}H5} = 1.0$, $H_{3Thienyl}$), 3.25 (m, 2H, $^aCH_2C=C$), 2.68 (m, 2H, $^bCH_2C=C$), 1.73 (m, 2H, $^aCH_2CH_2C=C$), 1.68 (m, 2H, $^bCH_2CH_2C=C$). ^{13}C NMR (600 MHz): 152.62 (s, C_2), 142.56 (s, C_6), 131.75 (s, C_7), 127.05 (s, C_4), 125.39 (s, C_3), 124.44 (s, C_5), 30.79 (s, C_8), 22.17 (s, C_9). MS: *m/z* 838.84 $[M+H]^+$, isotopic pattern peaks *m/z*: 836.82 ($^{187}Re\text{-}^{185}Re$), 838.84 ($^{185}Re\text{-}^{185}Re$) and 840.83 ($^{187}Re\text{-}^{187}Re$). UV−Vis: CH_2Cl_2, $\lambda_{max} = 234$ nm, $\varepsilon = 17384\ M^{-1}cm^{-1}$. Fluorescence: CH_2Cl_2, $\lambda_{max} = 549$ nm, $\Phi_f = 0.087$. Spectral data for **2a**: (cyclohexane, $\nu_{(CO)}/cm^{-1}$): 2042 m, 2012 s, 1962 m, 1930 w, 1928 w, 1912 w. ^1H NMR (500 MHz, $CDCl_3$): δ 7.15 (dd, 2H, $^3J_{H5\text{-}H4} = 5.3$ Hz, $^4J_{H5\text{-}H3} = 1.0$ Hz, $H_{5\ Thienyl}$), 6.99 (dd, 2H, $^3J_{H3\text{-}H4} = 3.3$ Hz, $^4J_{H3\text{-}H5} = 1.0$ Hz, $H_{4Thienyl}$), 6.79 (dd, 1H,$^3J_{H4\text{-}H5} = 5.31$ Hz, $^3J_{H4\text{-}H3} = 3.3$, $H_{3Thienyl}$), 3.20 (m, 2H, $^aCH_2C=C$), 2.76 (m, 2H, $^bCH_2C=C$), 2.49 (s, 3H, H_{CH3CN}), 1.85 (m, 2H, $^aCH_2CH_2C=C$), 1.65 (m, 2H, $^bCH_2CH_2C=C$). ^{13}C NMR (500 MHz, CD_2Cl_2): δ 193.8 (s, CO), 193.6 (s, CO), 186.2 (s, CO), 153.5 (s, C_2), 151.2 (s, C_6), 130.6 (s, C_7), 126.9 (s, C_3), 124.9 (s, C_4), 123.6 (s, C_5), 30.7 (s, C_8), 22.6 (s, C_9), 3.5 (C_{CH3CN}). MS: *m/z* 712.82 $[M\text{-}(CO)_5+H]^+$, isotopic pattern peaks *m/z*: 712.82 ($^{185}Re\text{-}^{187}Re$), 710.79 ($^{185}Re\text{-}^{185}Re$) and 714.81 ($^{187}Re\text{-}^{187}Re$). UV–Vis: CH_2Cl_2, $\lambda_{max} = 231$ nm, $\varepsilon = 18163\ M^{-1}cm^{-1}$. Fluorescence: CH_2Cl_2, $\lambda_{max} = 545$ nm, $\Phi_f = 0.06$.

4.3. Synthesis of $[Re_2(CO)_6(CH_3CN)_2(\mu\text{-}\eta^2{:}\eta^2\text{-}C_{18}H_{16}N_2)]$ (3b)

A solution of $[Re_2(CO)_8(CH_3CN)_2]$ (100 mg, 0.147 mmol) and 1,8-bis(2-pyridyl)octa-1,7-diyne (**b**) (38 mg, 0.147 mmol) in dry cyclohexane (25 mL) was refluxed under nitrogen for 4 h. After evaporation of the solvent, TLC (SiO_2, eluant: hexane/dichloromethane, 2:8 v/v) of the yellow residue gave one main band characterized as $[Re_2(CO)_6(CH_3CN)(\mu\text{-}\eta^1{:}\eta^1{:}\eta^2{:}\eta^2\text{-}C_{18}H_{16}N_2)]$ (**3b**) (47 mg; yield 36%). Spectral data for **3b**: IR (CH_2Cl_2, $\nu_{(CO)}/cm^{-1}$): 2036 m, 2007 m, 1949 m, 1919 s, 1896 s ^1H NMR (500 MHz, CD_2Cl_2): δ 8.51 (dd, 2H, $^3J_{H6\text{-}H5} = 4.8$ Hz, $^4J_{H6\text{-}H4} = 1.8$ Hz, $H_{6pyridyl}$), 7.64 (ddd, 2H, $^3J_{H4\text{-}H5} = 7.7$ Hz,$^3J_{H4\text{-}H3} = 7.7$ Hz, $^4J_{H4\text{-}H6} = 1.8$ Hz, $H_{4pyridyl}$), 7.14 (dd, 2H, $J_{H3\text{-}H4} = 7.7$ Hz, $J_{H3\text{-}H5} = 1.7$, $H_{3pyridyl}$), 7.04 (dd, 2H, $J_{H5\text{-}H4} = 7.7$ Hz, $J_{H5\text{-}H6} = 4.8$, $H_{5pyridyl}$), 3.13 (m, 2H, $^aCH_2C=C$), 2.44 (m, 2H, $^bCH_2C=C$), 2.12 (s, 3H, H_{CH3CN}), 1.75 (m, 2H, $^aCH_2CH_2C=C$), 1.68 (m, 2H, $^bCH_2CH_2C=C$). ^{13}C NMR (500 MHz, CD_2Cl_2): δ 165.8 (s, C_2), 156.0 (s, C_7), 149.7 (s, C_6), 136.3 (s, C_4), 129.7 (s, C_8), 121.5 (s, C_5), 121.2 (s, C_3), 31.0 (C_{CH3CN}), 30.4 (s, C_9), 22.4 (s, C_{10}). MS: *m/z* 836.31 $[M\text{-}(CH_3CN)_2+Cl]^-$, isotopic pattern peaks *m/z*: 836.31 ($^{185}Re\text{-}^{187}Re\text{-}^{35}Cl$), 838.30 ($^{187}Re\text{-}^{187}Re\text{-}^{35}Cl$) and 840.23 ($^{187}Re\text{-}^{187}Re\text{-}^{37}Cl$). UV−Vis: CH_2Cl_2, $\lambda_{max} = 298$ nm, $\varepsilon = 1828\ M^{-1}cm^{-1}$. Fluorescence: CH_2Cl_2, $\lambda_{max} = 599$ nm, $\Phi_f = 0.02$.

4.4. Synthesis of $[Re_2(CO)_6(CH_3CN)(\eta^1{:}\eta^1{:}\eta^2{:}\eta^2\text{-}C_{26}H_{20}N_2)]$ (2c) and $[Re_2(CO)_6(CH_3CN)_2(\eta^2{:}\eta^2\text{-}C_{26}H_{20}N_2)]$ (4c)

A mixture of $[Re_2(CO)_8(CH_3CN)_2]$ (100 mg; 0.147 mmol) and 8-di(2-quinolyl)octa-1,7-diyne (**c**) (53 mg; 0.147 mmol) in dry cyclohexane was stirred and refluxed for 6 h under nitrogen. The solvent was evaporated to dryness, and the solid residue was chromatographed by TLC (SiO_2, eluant: hexane/dichloromethane, 3:7 v/v) to give two compounds characterized as $[Re_2(CO)_6(CH_3CN)(\eta^1{:}\eta^1{:}\eta^2{:}\eta^2\text{-}C_{26}H_{20}N_2)]$ (**2c**) (51 mg; yield 74%) and $[Re_2(CO)_6(CH_3CN)_2(\eta^2{:}\eta^2\text{-}C_{26}H_{20}N_2)]$ (**4c**) (7 mg; yield 10%). Spectral data for **2c**: IR (CH_2Cl_2, $\nu_{(CO)}/cm^{-1}$): 2041 s, 2009 s, 1954 m, 1918 m, 1985 sh. ^1H NMR (600 MHz, CD_3COCD_3): δ 8.25 (d, 2H, $^3J_{H3\text{-}H4} = 8.4$ Hz, H_4), 8.02 (d, 2H, $^3J_{H8\text{-}H9} = 8.4$ Hz, H_9), 7.89 (d, 2H, $^3J_{H6\text{-}H7} = 7.9$ Hz, H_6), 7.70 (ddd, 2H, $^3J_{H8\text{-}H9} = 8.3$ Hz, $^3J_{H7\text{-}H8} = 6.9$ Hz, $^4J_{H6\text{-}H8} = 1.4$ Hz, H_8), 7.53 (m, 4H, $^3J_{H3\text{-}H4} = 8.4$ Hz, $^3J_{H6\text{-}H7} = 7.9$ Hz, $^3J_{H7\text{-}H8} = 6.9$ Hz, H_3, H_7), 3.31 (m, 2H, H_{13a}), 2.90 (s, 3H, H_{CH3CN}), 2.46 (m, 2H, H_{13b}), 1.82 (m, 4H, H_{14}). ^{13}C NMR (600 MHz, CD_3COCD_3): δ 194.8 (s, CO), 194. (s, CO), 186.9 (s, CO), 166.8 (s, C_2), 163.9 (s, C_5), 148.1 (s, C_{10}), 135.7 (s, C_4), 129.1 (s, C_8), 128.9 (s, C_{12}), 128.6 (s, C_9), 127.4 (s, C_6), 127.1 (s, C_{CH3CN}), 126.4 (s, C_{11}), 125.6 (s, C_7), 120.5 (s, C_3), 29.9 (s, C_{13}), 22.1 (s, C_{14}), 2.6 (s, C_{CH3CN}). MS: *m/z* 942.05 $[M+H]^+$, isotopic pattern peaks *m/z*: 942.05 ($^{187}Re\text{-}^{185}Re$), 940.26 ($^{185}Re\text{-}^{185}Re$) and 944.09 ($^{187}Re\text{-}^{187}Re$). UV−Vis: CH_2Cl_2, $\lambda_{max} = 230$ nm, $\varepsilon = 114960\ M^{-1}cm^{-1}$. Fluorescence: CH_2Cl_2, $\lambda_{max} = 408$ nm, $\Phi_f = 0.06$. Spectral data for **4c**: IR (CH_2Cl_2,$\nu_{(CO)}/cm^{-1}$): 2042 m, 2010 s, 1957 s, 1918 w. ^1H NMR (600 MHz, CD_2Cl_2): δ 8.23 (d, 2H, $^3J_{H3\text{-}H4} = 8.6$ Hz, H_4), 8.06 (dd, 4H, $^3J_{H3\text{-}H4} = 8.6$ Hz, $^3J_{H6\text{-}H7} = 9.0$ Hz, H_6, H_3), 7.82 (d, 2H, $^3J_{H8\text{-}H9} = 8.1$ Hz, H_9), 7.71 (ddd, 2H, $^3J_{H6\text{-}H7} = 9.0$ Hz, $^3J_{H7\text{-}H8} = 6.8$ Hz, $^3J_{H7\text{-}H9} = 1.4$ Hz, H_7), 7.51 (ddd, 2H, $^3J_{H8\text{-}H9} = 8.0$ Hz, $^3J_{H7\text{-}H8} = 6.9$ Hz, $^4J_{H6\text{-}H8}$ 1.1 Hz, H_8), 3.26 (s, 4H, H_{13}), 1.94 (m, 4H, H_{14}), 1.26 (s, 6H, H_{MeCN}). ^{13}C NMR (600 MHz, CD_2Cl_2): δ 151.0 (s, C_2), 148.8 (s, C_5), 147.3 (s, C_{11}), 136.5 (s, C_4), 130.0 (s, C_7), 129.6 (s, C_6), 128.0 (s, C_9), 127.9 (s, C_{12}), 126.3 (s, C_8), 118.4 (s, C_3), 30.1 (s, C_{CH3CN}), 24.1 (s, C_{13}), 23.4 (s, C_{14}). MS: *m/z* 980.63 $[M\text{-}H]^-$, isotopic pattern peaks *m/z*: 980.63 ($^{187}Re\text{-}^{185}Re$), 979.02 ($^{185}Re\text{-}^{185}Re$) and 982.02 ($^{187}Re\text{-}^{187}Re$). UV–Vis: CH_2Cl_2, $\lambda_{max} = 400$ nm, $\varepsilon = 20540\ M^{-1}cm^{-1}$. Fluorescence: CH_2Cl_2, $\lambda_{max} = 472$ nm, $\Phi_f = 0.64$.

4.5. *Synthesis of $[Re_2(CO)_6(CH_3CN)(\mu\text{-}\eta^1{:}\eta^1{:}\eta^2{:}\eta^2\text{-}C_{36}H_{26})]$ (**2d**)*

A mixture of $[Re_2(CO)_8(CH_3CN)_2]$ (100 mg; 0.147 mmol) and 1,8-bis(9-phenanthrenyl)octa-1,7-diyne (**d**) (68 mg; 0.147 mmol) in dry cyclohexane was refluxed under nitrogen for 2 h. After evaporation of the solvent, TLC (SiO_2, eluant: C_6H_{12}:CH_2Cl_2, 7:3 v/v) of the yellow residue gave one main band characterized as $[Re_2(CO)_6(CH_3CN)(\mu\text{-}\eta^1{:}\eta^1{:}\eta^2{:}\eta^2\text{-}C_{36}H_{26})]$ (**2d**) (18 mg; yield 17%). Spectral data for **2d**: IR (CH_2Cl_2, $\nu_{(CO)}/cm^{-1}$): 2039 m, 2008 s, 1950 s, 1924 w, 1889 sh. ^1H NMR (600 MHz, $CDCl_3$): δ 8.80 (d, 2H, $^3J_{H12\text{-}H13} = 8.2$ Hz, H_{13}), 8.63 (d, 2H, $^3J_{H6\text{-}H7} = 7.4$ Hz, H_7), 8.08 (d, 2H, $^3J_{H4\text{-}H5} = 8.1$ Hz, H_4), 7.92 (m, 2H, H_{10}), 7.88 (s, 2H, H_2), 7.66 (dd, 2H, $^3J_{H12\text{-}H13} = 8.2$ Hz, $^3J_{H11\text{-}H12} = 7.5$ Hz, H_{12}), 7.63 (m, 6H, H_{11}, H_5, H_6), 3.08 (m, 2H, H_{17a}), 2.57 (m, 2H, H_{17b}), 2.38 (s, 3H, H_{CH3CN}), 1.88 (m, 2H, H_{18a}), 1.68 (m, 2H, H_{18b}). ^{13}C NMR (600 MHz, $CDCl_3$): δ 194.8 (s, CO), 193.9 (s, CO), 187.7 (s, CO), 162.9 (s, C_{15}), 145.4 (s, C_8), 132.5 (s, C_9), 131.2 (s, C_1), 129.7 (s, C_{16}), 128.8 (s, C_{14}), 128.6 (s, C_{10}), 127.5 (s, C_3), 127.4 (s, C_2), 127.0 (s, C_{11}), 126.3 (s, C_4), 126.1 (s, C_{12}), 125.7–124.6 (s, C_5, C_6), 124.1 (s, C_{13}), 122.2 (s, C_7), 30.8 (s, C_{17}), 22.3 (s, C_{18}), 4.3 (s, C_{CH3CN}). MS: *m/z* 1074.15 $[M + Cl\text{-}H]^-$, isotopic pattern peaks *m/z*: 1072.08 ($^{187}Re\text{-}^{185}Re\text{-}^{35}Cl$), 1074.09 ($^{187}Re\text{-}^{187}Re\text{-}^{35}Cl$) and 1076.08 ($^{187}Re\text{-}^{187}Re\text{-}^{37}Cl$). UV–Vis: CH_2Cl_2, $\lambda_{max} = 250$ nm, $\varepsilon = 54300\ M^{-1}cm^{-1}$. Fluorescence: CH_2Cl_2, $\lambda_{max} = 428$ nm, $\Phi_f = 0.03$.

4.6. *Crystal structure determination*

Data collections were performed in a Bruker APEX II CCD diffractometer using Mo Kα (λ = 0.71703 Å) radiation and the APEX2 software (Bruker, 2010). Cell refinement and data reduction were performed in SAINT (Bruker, 2010) and SHELXT [84] and SHELXL [85] were used for solution and refinement of the structures. All the refinement process was performed with OLEX2 [86] which was also used to prepare molecular graphics for publication. All non-hydrogen atoms were refined anisotropically, including those in disorder. Hydrogen atoms were modelled in idealized positions and refined according to the riding model. Further crystallographic information is available as supporting information as well as CCDC files (1831209, 1831210, 1831211). These data can be obtained free of charge via http://www.ccdc.cam.ac.uk/conts/retrieving.html (or from the CCDC, 12 Union Road, Cambridge CB2 1EZ, UK; fax, + 44 1223 336033; e-mail, deposit@ccdc.cam.ac.uk).

4.7. *Theoretical calculations*

DFT and TD-DFT calculations were performed in the ORCA package (version 4.0.1) [87] using the PBE0 hybrid functional [88] and the def2-SVP basis set for all atoms [89]. Inclusion of relativistic effects was necessary to account for correct bond distances involving the metal atoms like previously reported [90–94]. The quasi-relativistic Stuttgart-Dresden ECP was used for rhenium in all calculations [95]. Built-in auxiliary basis sets were employed together with the RIJCOSX approximation [95]. Convergence criteria for geometries were 5.0×10^{-6} E_h for the energy change and a RMS gradient of 1.0×10^{-4} $E_h\ a_0^{-1}$. In all cases, the densities were optimized using a DIIS procedure with a tolerance for the energy of 1.0×10^{-8} E_h. TD-DFT calculations were used to obtain vertical excitations using the same level of theory. For all complexes, the first 50 singlet excited states were calculated using a 2.5×10^{-7} E_h as the convergence tolerance for the energies. Comparison between theoretical and experimental (XRD) structures was performed by superimposing two structures considering coincident centers of mass. The overlay was optimized using rotation matrices in order to minimize the root mean squared deviation.

Acknowledgements

We thank the Instituto Venezolano de Investigaciones Científicas for financial support (Project No 1082). The authors thank Dr. Tamara Zoltan and William Castro for allowing us to use the UV–Vis and fluorescence spectrometers of their laboratories at the IVIC. We thank Fundação de Amparo à Pesquisa do Estado de São Paulo - FAPESP (grant nr. 2013/22127-2), INOMAT - INCT for Science, Technology and Innovation in Functional Complex Materials (grant nr. 2014/50906-9) and Conselho Nacional de Desenvolvimento Científico e Tecnológico – CNPq (grant nr. 310779/2016-2) for financial support and also Centro Nacional de Processamento de Alto Desempenho em São Paulo – CENAPAD-SP for computational facilities in which all DFT calculations were performed.

Appendix A. Supplementary data

NMR, FT-IR, and MS spectra of new compounds and computational details of compounds are found in supplementary material.

Supplementary data to this article can be found online at https://doi.org/10.1016/j.jorganchem.2018.12.003.

References

[1] E.J. Meijer, C. Tanase, P.W.M. Blom, E. Van Veenendaal, B.-H. Huisman, D.M. De Leeuw, T.M. Klapwijk, Switch-on voltage in disordered organic field-effect transistors, Appl. Phys. Lett. 80 (2002) 3838–3840.
[2] A.R. Brown, A. Pomp, C.M. Hart, D.M. De Leeuw, Logic gates made from polymer transistors and their use in ring oscillators, Science (80-.) 270 (1995) 972–974.
[3] M. Goes, J.W. Verhoeven, H. Hofstraat, K. Brunner, OLED and PLED devices employing electrogenerated, intramolecular charge-transfer fluorescence, ChemPhysChem 4 (2003) 349–358.
[4] R. Badugu, J.R. Lakowicz, C.D. Geddes, Enhanced fluorescence cyanide detection at physiologically lethal levels: reduced ICT-based signal transduction, J. Am. Chem. Soc. 127 (2005) 3635–3641.
[5] F. Yukruk, E.U. Akkaya, Modulation of internal charge transfer (ICT) in a bay region hydroxylated perylenediimide (PDI) chromophore: a chromogenic chemosensor for pH, Tetrahedron Lett. 46 (2005) 5931–5933.
[6] A.N. Swinburne, M.J. Paterson, A. Beeby, J.W. Steed, Fluorescent 'Twist-on'sensing by induced-fit anion stabilisation of a planar chromophore, Chem. Eur J. 16 (2010) 2714–2718.
[7] W. Rettig, Charge separation in excited states of decoupled systems—TICT compounds and implications regarding the development of new laser dyes and the primary process of vision and photosynthesis, Angew Chem. Int. Ed. Engl. 25 (1986) 971–988.
[8] S. Durben, D. Nickel, R.A. Krüger, T.C. Sutherland, T. Baumgartner, Toward low-band gap dithienophosphole copolymers for an application in organic solar cells, J. Polym. Sci. Part A Polym. Chem. 46 (2008) 8179–8190.
[9] S. Günes, H. Neugebauer, N.S. Sariciftci, Conjugated polymer-based organic solar cells, Chem. Rev. 107 (2007) 1324–1338.
[10] A. Kraft, A.C. Grimsdale, A.B. Holmes, Electroluminescent conjugated polymersÐseeing polymers in a new light, Angew. Chem. Int. End Engl. 37 (1998) 402–428.
[11] A. Arcadi, S. Cacchi, F. Marinelli, Palladium-catalysed coupling of aryl and vinyl triflates or halides with 2-ethynylaniline: An efficient route to functionalized 2-substituted indoles, Tetrahedron Lett. 30 (1989) 2581–2584.
[12] K. Okuro, M. Furuune, M. Enna, M. Miura, M. Nomura, Synthesis of aryl-and vinylacetylene derivatives by copper-catalyzed reaction of aryl and vinyl iodides with terminal alkynes, J. Org. Chem. 58 (1993) 4716–4721.
[13] R.C. Larock, E.K. Yum, M.J. Doty, K.K.C. Sham, Synthesis of aromatic heterocycles via palladium-catalyzed annulation of internal alkynes, J. Org. Chem. 60

(1995) 3270–3271.

[14] M.W. Miller, C.R. Johnson, Sonogashira coupling of 2-iodo-2-cycloalkenones: synthesis of (+)-and (−)-harveynone and (−)-tricholomenyn A, J. Org. Chem. 62 (1997) 1582–1583.

[15] J.W. Grissom, G.U. Gunawardena, D. Klingberg, D. Huang, The chemistry of enediynes, enyne allenes and related compounds, Tetrahedron 52 (1996) 6453–6518.

[16] M.E. Maier, Design of enediyne prodrugs, Synlett 1995 (1995) 13–26.

[17] M. Gholami, R.R. Tykwinski, Oligomeric and polymeric systems with a cross-conjugated π-framework, Chem. Rev. 106 (2006) 4997–5027.

[18] J. Liu, J.W.Y. Lam, B.Z. Tang, Acetylenic polymers: syntheses, structures, and functions, Chem. Rev. 109 (2009) 5799–5867.

[19] M. Murai, E. Uemura, S. Hori, K. Takai, Rhenium-catalyzed construction of polycyclic hydrocarbon frameworks by a unique cyclization of 1, n-diynes initiated by 1,1-difunctionalization with carbon nucleophiles, Angew. Chem. 129 (2017) 5956–5960.

[20] S. Yasuike, J. Kurita, T. Tsuchiya, Syntheses of novel group 15 and 16 thieno [2,3-b]-, thieno [3,4-b]-, and thieno [3,2-b]-heteroles, Heterocycles 10 (1997) 1891–1894.

[21] E. Sappa, A. Tiripicchio, P. Braunstein, Alkyne-substituted homo-and hetero-metallic carbonyl clusters of the iron, cobalt and nickel triads, Chem. Rev. 83 (1983) 203–239.

[22] J.F. Corrigan, S. Doherty, N.J. Taylor, A.J. Carty, Tailored synthesis of hydrocarbon chains via carbon-carbon coupling reactions of diynes and alkynes on the square face of a ruthenium Ru_4P cluster, Organometallics 11 (1992) 3160–3163.

[23] S.P. Tunik, E. V Grachova, V.R. Denisov, G.L. Starova, A.B. Nikol'skii, F.M. Dolgushin, A.I. Yanovsky, Y.T. Struchkov, Reactions of diacetylene ligands with trinuclear clusters II. Reactions of hexa-2,4-diyne-1,6-diol and 1,4-diphenyl-1,3-butadiyne with $Ru_3(CO)_{12}$, J. Organomet. Chem. 536 (1997) 339–343.

[24] Q. Lin, W.K. Leong, L. Gao, The photochemical and thermal reactions of a triosmium cluster carrying a γ-pyrone ligand with alkynes, J. Organomet. Chem. 689 (2004) 25–34. https://doi.org/10.1016/j.jorganchem.2003.09.022.

[25] C.J. Adams, L.P. Clarke, A.M. Martín-Castro, P.R. Raithby, G.P. Shields, A new two-strand chain cluster: the synthesis and characterisation of $[Os_3(CO)_{11}\{\mu^3\text{-}\eta^4\text{-}(C_4H_3S)C_2C_2(C_4H_3S)\}]$, J. Chem. Soc., Dalton Trans. (2000) 4015–4017, https://doi.org/10.1039/B006696F.

[26] M.I. Alcalde, A.J. Carty, Y. Chi, E. Delgado, B. Donnadieu, E. Hernández, K. Dallmann, J. Sánchez-Nieves, Syntheses of new ruthenium clusters containing sulfur, ynyl and diynyl ligands. Crystal structures of $[Ru_3(CO)_9(\mu\text{-}\eta^2\text{-}SC{\equiv}CSiMe3)(\mu_3\text{-}\eta^2\text{-}C{\equiv}CSiMe3)]$, $[Ru_4(CO)_{12}(\mu_4\text{-}S)(\mu\text{-}\eta^2\text{-}C{\equiv}CSiMe_3)_2]$ and $[Ru_4(CO)_9(\mu\text{-}CO)_2(\mu4\text{-}S)(\mu_4\text{-}\eta^2\text{-}C(SiMe_3)C(C{\equiv}CSiMe_3)]$, J. Chem. Soc., Dalton Trans. (2001) 2502–2507, https://doi.org/10.1039/B103202J.

[27] T.-W. Shiue, W.-Y. Yeh, G.-H. Lee, S.-M. Peng, Complexation and metallation of $Ph_2PCC(CH_2)_5CCPh_2$ in triosmium carbonyl clusters, J. Organomet. Chem. 692 (2007) 3619–3624. https://doi.org/10.1016/j.jorganchem.2007.05.003.

[28] G. Gervasio, E. Sappa, A. Secco, Advances in the chemistry of alkyne-substituted homo- and heterometallic carbonyl clusters of the iron, cobalt and nickel triads. An update, J. Organomet. Chem. 751 (2014) 111–152. https://doi.org/10.1016/j.jorganchem.2013.08.046.

[29] D.B. Pourreau, R.R. Whittle, G.L. Geoffroy, Dirhenium complexes containing linked diphenylacetylene molecules from the photoreaction of $H_3Re_3(CO)_{12}$ with $PhC{\equiv}CPh$. Crystal and molecular structures of $Re_2(CO)_5(C_4Ph_4)(C_4Ph_4)$ and $Re_2(CO)_4$ $(C_6Ph_6)(C_2Ph_2{\cdot}12$ hexane), J. Organomet. Chem. 273 (1984) 333–346.

[30] M.J. Mays, D.W. Prest, P.R. Raithby, Dirhenium complexes containing two, three, and four linked acetylene molecules derived from the reaction of $[Re_2(CO)_{10}]$ with RC_2R (R= Ph or Me); the X-ray crystal structure of $[Re_2(CO)_4\{(PhCCPh)_3\}(CNCH_2\ SO_2C_6H_4Me\text{-}p)_2]{\cdot}CH_2Cl_2$, J. Chem. Soc., Dalton Trans. (1981) 771–776.

[31] A.A. Koridze, V.I. Zdanovlch, A.S. Batsanov, Y.T. Struchkov, Annelation of Phenylacetylide Groups by Thermolysis of $(OC)_5ReCCPh$. X-Ray Crystal Structure of $Re_2(CO)_7(C_2Ph)_4$, Mendeleev Commun. 1 (1991) 126–127.

[32] A.A. Koridze, V.I. Zdanovich, O.A. Kizas, A.I. Yanovsky, Y.T. Struchkov, Coupling and annelation of two acetylide groups and alkyne molecules in the reaction of $(OC)\ _5ReC{\equiv}CPh$ with ferrocenylacetylene. Crystal and molecular structure of $Re_2(CO)_7$ $\{C_8H_2Ph_2(C_5H_4FeC_5H_5)_2\}{\cdot}$acetone, J. Organomet. Chem. 464 (1994) 197–201.

[33] M.I. Bruce, P.J. Low, B.W. Skelton, A.H. White, Rhenium complexes from alkynes. X-Ray crystal structures of $Re_2(\mu\text{-}_2\eta^1,\text{-}C_4Ph_4)(CO)_7$ and $Re\{C,O\text{-}CH{\equiv}C$ $[Re(CO)_4$ $(NMe_3)]C(OMe)O\}(CO)_4$, J. Organomet. Chem. 464 (1994) 191–195.

[34] W. Ma, C. Yu, T. Chen, L. Xu, W.-X. Zhang, Z. Xi, Metallacyclopentadienes: synthesis, structure and reactivity, Chem. Soc. Rev. 46 (2017) 1160–1192.

[35] R.D. Adams, G. Chen, J. Yin, Clusters containing ynamine ligands. 3. Syntheses and structural characterizations of $Re_2(CO)_8$(.mu.-MeC_2NMe_2) and $Re_2(CO)_7$[.mu.-C $(Me)C(NMe_2)C(NMe_2)C(Me)$], Organometallics 10 (1991) 1278–1282.

[36] A.A. Hock, O.S. Mills, Studies of some carbon compounds of the transition metals. II. The structure of $MeC{:}CMe.H_2F_2(CO)_8$, Acta Crystallogr. 14 (1961) 139–148.

[37] X. Yan, C. Xi, Conversion of zirconacyclopentadienes into metalloles: Fagan–Nugent reaction and beyond, Acc. Chem. Res. 48 (2015) 935–946.

[38] T. Takahashi, Y. Li, Zirconacyclopentadienes in organic synthesis, Titan. Zircon. Org. Synth. (2002) 50–85.

[39] H. Bönnemann, Organocobalt Compounds in the Synthesis of Pyridines—An Example of Structure-Effectivity Relationships in Homogeneous Catalýsis, Angew Chem. Int. Ed. Engl. 24 (1985) 248–262.

[40] D.P. Hsu, W.M. Davis, S.L. Buchwald, Synthesis and structure of seven-membered cyclic cumulene, J. Am. Chem. Soc. 115 (1993) 10394–10395, https://doi.org/10.1021/ja00075a079.

[41] V.V. Burlakov, A. Ohff, C. Lefeber, A. Tillack, W. Baumann, R. Kempe, U. Rosenthal, The First Titanacyclic Five-Membered Cumulene. Synthesis, Structure, and Reactivity, Chem. Ber. 128 (1995) 967–971.

[42] M.I. Bruce, N.N. Zaitseva, B.W. Skelton, A.H. White, Reactions between ruthenium cluster carbonyls and 1,4-diphenylbuta-1,3-diyne, Inorg. Chim. Acta. 250 (1996) 129–138.

[43] U. Rosenthal, P.-M. Pellny, F.G. Kirchbauer, V. V Burlakov, What do titano-and zirconocenes do with diynes and polyynes? Acc. Chem. Res. 33 (2000) 119–129.

[44] J.P. Rourke, A.S. Batsanov, J.A.K. Howard, T.B. Marder, Regiospecific high yield reductive coupling of diynes to give a luminescent rhodium complex, Chem. Commun. (2001) 2626–2627, https://doi.org/10.1039/B108625A.

[45] J.M. Burke, R.B. Coapes, A.E. Goeta, J.A.K. Howard, T.B. Marder, E.G. Robins, S.A. Westcott, Synthesis, characterisation and molecular structure of $[Rh(COE)_2(acac)]$ (COE = cyclooctene, $\eta^2\text{-}C_8H_{14}$), an important starting material for the preparation of rhodium catalyst precursors, J. Organomet. Chem. 649 (2002) 199–203.

[46] M. Horáček, I. Císařová, J. Kubišta, A. Spannenberg, K. Dallmann, U. Rosenthal, K. Mach, Titanocene—1,4,6-tris(trimethylsilyl)hex-3-ene-1,5-diyne-3-yl complexes—crystal structures and their retro reaction, J. Organomet. Chem. 689 (2004) 4592–4600.

[47] A.F. Hill, A.D. Rae, M. Schultz, A.C. Willis, Bis (alkynyl), metallacyclopentadiene, and diphenylbutadiyne complexes of ruthenium, Organometallics 26 (2007) 1325–1338.

[48] B. Heller, M. Hapke, The fascinating construction of pyridine ring systems by transition metal-catalysed [2+2+2] cycloaddition reactions, Chem. Soc. Rev. 36 (2007) 1085–1094.

[49] J. Wei, Y. Zhang, W. Zhang, Z. Xi, 1, 3-butadienyl dianions as non-innocent ligands: synthesis and characterization of aromatic dilithio rhodacycles, Angew. Chem. Int. Ed. 54 (2015) 9986–9990.

[50] C. Sieck, M.G. Tay, M. Thibault, R.M. Edkins, K. Costuas, J. Halet, A.S. Batsanov, M. Haehnel, K. Edkins, A. Lorbach, Reductive coupling of diynes at rhodium gives fluorescent rhodacyclopentadienes or phosphorescent rhodium 2,2'-biphenyl complexes, Chem. Eur J. 22 (2016) 10523–10532.

[51] A. Steffen, M.G. Tay, A.S. Batsanov, J.A.K. Howard, A. Beeby, K.Q. Vuong, X.-Z. Sun, M.W. George, T.B. Marder, 2,5-bis(p-R-arylethynyl)rhodacyclopentadienes show intense fluorescence: denying the presence of a heavy atom, Angew. Chem. Int. Ed. 49 (2010) 2349–2353, https://doi.org/10.1002/anie.200905697.

[52] Y.Y. Chia, M.G. Tay, An insight into fluorescent transition metal complexes, Dalton Trans. 43 (2014) 13159–13168, https://doi.org/10.1039/C4DT01098A.

[53] A. Steffen, K. Costuas, A. Boucekkine, M.-H. Thibault, A. Beeby, A.S. Batsanov, A. Charaf-Eddin, D. Jacquemin, J.-F. Halet, T.B. Marder, Fluorescence in rhoda-and iridacyclopentadienes neglecting the spin—orbit coupling of the heavy atom: the ligand dominates, Inorg. Chem. 53 (2014) 7055–7069, https://doi.org/10.1021/ic501115k.

[54] A. Steffen, R.M. Ward, M.G. Tay, R.M. Edkins, F. Seeler, M. van Leeuwen, L.-O. Pålsson, A. Beeby, A.S. Batsanov, J.A.K. Howard, T.B. Marder, Regiospecific formation and unusual optical properties of 2,5-bis(arylethynyl)rhodacyclopentadienes: a new class of luminescent organometallics, Chem. Eur J. 20 (2014) 3652–3666, https://doi.org/10.1002/chem.201304068.

[55] C. Sieck, D. Sieh, M. Sapotta, M. Haehnel, K. Edkins, A. Lorbach, A. Steffen, T.B. Marder, Convenient synthetic access to fluorescent rhodacyclopentadienes via ligand exchange reactions, J. Organomet. Chem. 847 (2017) 184–192, https://doi.org/10.1016/J.JORGANCHEM.2017.02.028.

[56] A. Steffen, R.M. Ward, M.G. Tay, R.M. Edkins, F. Seeler, M. van Leeuwen, L. Pålsson, A. Beeby, A.S. Batsanov, J.A.K. Howard, Regiospecific formation and unusual optical properties of 2,5-bis(arylethynyl)rhodacyclopentadienes: a new class of luminescent organometallics, Chem. Eur J. 20 (2014) 3652–3666.

[57] A. Steffen, M.G. Tay, A.S. Batsanov, J.A.K. Howard, A. Beeby, K.Q. Vuong, X. Sun, M.W. George, T.B. Marder, 2,5-bis(p-R-arylethynyl)rhodacyclopentadienes show intense fluorescence: denying the presence of a heavy atom, Angew. Chem. 122 (2010) 2399–2403.

[58] A.M. Stolzenberg, E.L. Muetterties, Mechanisms of dirhenium decacarbonyl substitution reactions: crossover experiments with dirhenium-185 decacarbonyl and dirhenium-187 decacarbonyl, J. Am. Chem. Soc. 105 (1983) 822–827.

[59] K.W. Lee, T.L. Brown, Photochemical reactions of $Re_2(CO)_9L$, 1,2-$Re_2(CO)_8L_2$, and $Re_2(CO)_8$(.mu.-LL) with alkenes, Organometallics 4 (1985) 1030–1036.

[60] M.I. Bruce, P.J. Low, B.W. Skelton, A.H. White, Some chemistry of $Re_2(\mu\text{-}H)(\mu\text{-}C_2Ph)(CO)_8$: X-ray structures of $Re_2(\mu\text{-}H)(\mu\text{-}C_2Ph)(CO)_6(PMe_3)_2$, $Re_2\{\mu\text{-}Au(PPh_3)\}(\mu\text{-}C_2Ph)(CO)_8$, $Re_2(\mu\text{-}X)(\mu\text{-}dppm)(\mu\text{-}C_2Ph)(CO)_6$ [X= H, Br and $Au(PPh_3)$] and $Re_2(\mu\text{-}Br)_2(\mu\text{-}dppm)(CO)_6$, J. Organomet. Chem. 515 (1996) 65–79.

[61] K.W. Lee, W.T. Pennington, A.W. Cordes, T.L. Brown, Bridging phosphorus ligand substituted dirhenium octacarbonyl compounds. Preparation and reactions with water and methanol, Organometallics 3 (1984) 404–413.

[62] E.F. Day, T.A. Payne, C.A. Holt, Mass spectrometric study of dirhenium bis-carboxylate: purine dinucleotide complexes, Rapid Commun. Mass Spectrom.

21 (2007) 903–910.

[63] A. Steffen, R.M. Ward, W.D. Jones, T.B. Marder, Dibenzometallacyclopentadienes, boroles and selected transition metal and main group heterocyclopentadienes: Synthesis, catalytic and optical properties, Coord. Chem. Rev. 254 (2010) 1950–1976.

[64] W.L. Ingham, N.J. Coville, Site selectivity studies on homonuclear metal dimer complexes: Substitution reactions of Re$_2$(CO)$_9$L, J. Organomet. Chem. 423 (1992) 51–64. https://doi.org/10.1016/0022-328X(92)83023-B.

[65] P.J. Giordano, S.M. Fredericks, M.S. Wrighton, D.L. Morse, Simultaneous multiple emissions from fac-XRe(CO)$_3$(3-benzoylpyridine)$_2$:n-.pi.* intraligand and charge-transfer emission at low temperature, J. Am. Chem. Soc. 100 (1978) 2257–2259.

[66] S.M. Fredericks, J.C. Luong, M.S. Wrighton, Multiple emissions from rhenium (I) complexes: intraligand and charge-transfer emission from substituted metal carbonyl cations, J. Am. Chem. Soc. 101 (1979) 7415–7417.

[67] W.K. Smothers, M.S. Wrighton, Raman spectroscopy of electronic excited organometallic complexes: a comparison of the metal to 2,2'-bipyridine charge-transfer state of fac-(2,2'-bipyridine) tricarbonylhalorhenium and tris (2,2'-bipyridine) ruthenium (II), J. Am. Chem. Soc. 105 (1983) 1067–1069.

[68] L. Sacksteder, A.P. Zipp, E.A. Brown, J. Streich, J.N. Demas, B.A. DeGraff, Luminescence studies of pyridine.alpha.-diimine rhenium (I) tricarbonyl complexes, Inorg. Chem. 29 (1990) 4335–4340.

[69] R.M. Leasure, L. Sacksteder, D. Nesselrodt, G.A. Reitz, J.N. Demas, B.A. DeGraff, Excited-state acid-base chemistry of (.alpha.-diimine) cyanotricarbonylrhenium (I) complexes, Inorg. Chem. 30 (1991) 3722–3728.

[70] S. Van Wallendael, R.J. Shaver, D.P. Rillema, B.J. Yoblinski, M. Stathis, T.F. Guarr, Ground-state and excited-state properties of monometallic and bimetallic complexes based on rhenium (I) tricarbonyl chloride: effect of an insulating vs a conducting bridge, Inorg. Chem. 29 (1990) 1761–1767.

[71] P.J. Giordano, M.S. Wrighton, The nature of the lowest excited state in fac-tricarbonylhalobis (4-phenylpyridine) rhenium (I) and fac-tricarbonylhalobis(4,4'-bipyridine) rhenium (I): emissive organometallic complexes in fluid solution, J. Am. Chem. Soc. 101 (1979) 2888–2897.

[72] S.R. Stoyanov, J.M. Villegas, D.P. Rillema, Time-dependent density functional theory study of the spectroscopic properties related to aggregation in the platinum (II) biphenyl dicarbonyl complex, Inorg. Chem. 42 (2003) 7852–7860.

[73] Y.-M. Cheng, Y.-S. Yeh, M.-L. Ho, P.-T. Chou, P.-S. Chen, Y. Chi, Dual room-temperature fluorescent and phosphorescent emission in 8-quinolinolate osmium (II) carbonyl complexes: Rationalization and generalization of intersystem crossing dynamics, Inorg. Chem. 44 (2005) 4594–4603.

[74] S.W. Buckner, M.J. Fischer, P.A. Jelliss, R. Luo, S.D. Minteer, N.P. Rath, A. Siemiarczuk, Dual fluorescence from an isonido Re^{III} rhenacarborane phosphine complex, [7,10-μ-H-7-CO-7,7-(PPh$_3$)2-isonido-7,8,9-ReC$_2$B$_7$H$_9$], Inorg. Chem. 45 (2006) 7339–7347.

[75] Y. Koga, K. Ueno, K. Matsubara, New preparative procedure for photoluminescent metallopolymers having a biphenyl-2,2′-diyl iridium (III) unit bound to a phosphine copolymer ligand, J. Polym. Sci. Part A Polym. Chem. 44 (2006) 4204–4213.

[76] K.R. Lee, M.-S. Eum, C.S. Chin, S.C. Lee, I.J. Kim, Y.S. Kim, Y. Kim, S.-J. Kim, N.H. Hur, New heteroleptic iridium complexes having one biphenyl-2,2′-diyl and two bipyridyl based ligands, Dalton Trans. (2009) 3650–3652.

[77] P.G. Bomben, K.C.D. Robson, B.D. Koivisto, C.P. Berlinguette, Cyclometalated ruthenium chromophores for the dye-sensitized solar cell, Coord. Chem. Rev. 256 (2012) 1438–1450.

[78] C.-C. Hsu, C.-C. Lin, P.-T. Chou, C.-H. Lai, C.-W. Hsu, C.-H. Lin, Y. Chi, Harvesting highly electronically excited energy to triplet manifolds: state-dependent intersystem crossing rate in Os (II) and Ag (I) complexes, J. Am. Chem. Soc. 134 (2012) 7715–7724.

[79] R. Czerwieniec, M.J. Leitl, H.H.H. Homeier, H. Yersin, Cu (I) complexes–Thermally activated delayed fluorescence. Photophysical approach and material design, Coord. Chem. Rev. 325 (2016) 2–28.

[80] W.L.F. Armarego, Purification of laboratory chemicals, Butterworth-Heinemann, 2017.

[81] Y. Otero, W. Vera, Y. León, C. Cardozo, D. Peña, A. Arce, Y. De Sanctis, T. Gonzalez, Synthesis, crystal structures and properties of 1,8-di(quinol-2-yl) octa-1,7-diyne and 1,8-di(phenantren-9-yl)octa-1,7-diyne, J. Chem. Res. 39 (2015) 48–52.

[82] M.I. Bruce, P.J. Low, Expeditious synthesis of Re$_3$(μ-H)$_3$(CO)$_{11}$(NCMe), J. Organomet. Chem. 519 (1996) 221–222.

[83] C. Hay, M. Hissler, C. Fischmeister, J. Rault-Berthelot, L. Toupet, L. Nyulászi, R. Réau, Phosphole-Containing π-Conjugated Systems: from model molecules to polymer films on electrodes, Chem. Eur J. 7 (2001) 4222–4236.

[84] G.M. Sheldrick, SHELXT–Integrated space-group and crystal-structure determination, Acta Crystallogr. Sect. A Found. Adv. 71 (2015) 3–8.

[85] G.M. Sheldrick, Crystal structure refinement with SHELXL, Acta Crystallogr. Sect. C Struct. Chem. 71 (2015) 3–8.

[86] O. V Dolomanov, L.J. Bourhis, R.J. Gildea, J.A.K. Howard, H. Puschmann, OLEX2: a complete structure solution, refinement and analysis program, J. Appl. Crystallogr. 42 (2009) 339–341.

[87] F. Neese, The ORCA program system, Wiley Interdiscip. Rev. Comput. Mol. Sci. 2 (2012) 73–78.

[88] C. Adamo, V. Barone, Toward reliable density functional methods without adjustable parameters: The PBE0 model, J. Chem. Phys. 110 (1999) 6158–6170.

[89] F. Weigend, R. Ahlrichs, PCCP 2005, 7, 3297, CrossRef| PubMed| CAS| Web Sci. Times Cited. 1396 (n.d.).

[90] M.A. Carvalho, R.E. de Paiva, F.R. Bergamini, A.F. Gomes, F.C. Gozzo, W.R. Lustri, A.L. Formiga, S.M. Shishido, C.V. Ferreira, P.P. Corbi, A silver complex with tryptophan: Synthesis, structural characterization, DFT studies and antibacterial and antitumor assays in vitro, J. Mol. Struct. 1031 (2013) 125–131.

[91] C. Abbehausen, T.A. Heinrich, E.P. Abrao, C.M. Costa-Neto, W.R. Lustri, A.L.B. Formiga, P.P. Corbi, Chemical, spectroscopic characterization, DFT studies and initial pharmacological assays of a silver (I) complex with N-acetyl-L-cysteine, Polyhedron 30 (2011) 579–583.

[92] G.S.M. Costa, P.P. Corbi, C. Abbehausen, A.L.B. Formiga, W.R. Lustri, A. Cuin, Silver (I) and gold (I) complexes with penicillamine: Synthesis, spectroscopic characterization and biological studies, Polyhedron 34 (2012) 210–214.

[93] M.A. Carvalho, B.C. Souza, R.E.F. Paiva, F.R.G. Bergamini, A.F. Gomes, F.C. Gozzo, W.R. Lustri, A.L.B. Formiga, G. Rigatto, P.P. Corbi, Synthesis, spectroscopic characterization, DFT studies, and initial antibacterial assays in vitro of a new palladium (II) complex with tryptophan, J. Coord. Chem. 65 (2012) 1700–1711.

[94] D. Andrae, U. Haeussermann, M. Dolg, H. Stoll, H. Preuss, Energy-adjustedab initio pseudopotentials for the second and third row transition elements, Theor. Chim. Acta 77 (1990) 123–141.

[95] R. Izsák, F. Neese, An overlap fitted chain of spheres exchange method, J. Chem. Phys. 135 (2011) 144105.